This is the accepted version of a paper published in 8th Conference on Ammonia and CO2 Refrigeration Technologies
DOI: 10.18462/iir.nh3-co2.2019.0041

A CFD analysis for the performance assessment of a novel design of plates-in-tank latent storage unit for freezing applications

Håkon SELVNES[(a)], Yosr ALLOUCHE[(a)], Alexis SEVAULT[(b)] , Armin HAFNER[(a)]

[(a)] Norwegian University of Science and Technology, Department of Energy and Process Engineering Trondheim, NO-7034, Norway, hakon.selvnes@ntnu.no
[(b)]SINTEF Energy Research, NO-7465 Trondheim, Norway

ABSTRACT

In this paper, the charging and discharging processes of a recently developed cold thermal energy storage (CTES) unit integrated into a poultry processing plant is investigated. A mathematical model of the CTES was created based on the two-dimensional transient Navier-Stokes equations using the ANSYS Fluent commercial software package. Thermal storage is commonly designed either for full storage (to meet the entire needs during peak hours) or for partial storage (to meet a fraction of the needs when there is a time shift between the energy supply and demand). In this study, the storage unit is designed to operate in a full storage operational mode integrated in the R744 circuit of a R717/R744 cascade refrigeration system. The CTES unit consists of a stack of heat exchanger (HEX) plates immersed in a steel tank filled with a phase change material (PCM). The selection of the appropriate PCM is based on the operational temperature range required in the system. Water is chosen as the PCM for this study. It is characterised by a high energy storage density and well-defined thermal properties. The HEX plates are called pillow plates (PP-HEX), and consists of two spot-welded and inflated steel plates that allows the CO_2 to circulate in a specific pattern and enhance the heat transfer. The CO_2 circulates within the plates to freeze and melt the PCM during the charging and discharging processes, respectively. The pressure-based model was selected to model the phase change based on the enthalpy-porosity formulation. This study aims to evaluate the relevance of detailed modelling of the PP-HEX structure compared to flat walls for the melting/solidification process. Results show that the flat wall model have comparable melting/solidification time and heat transfer rate to the PP-HEX geometry.

Keywords: Carbon dioxide, Cold thermal energy storage, Phase change material, CFD

1. INTRODUCTION

Natural refrigerants such as ammonia, hydrocarbons and CO_2 are becoming increasingly popular due to their favorable thermo-physical properties, low environmental impact and affordable cost (Lorentzen, 1995) (Nekså et al., 2010). Industrial refrigeration systems are commonly installed in applications where the difference in the peak and the average cooling load is substantial. CTES integrated into refrigeration systems allow for the load shifting from peak hours to off-peak hours. This operational mode will require more investment costs, but would generate important energy savings. In order to reduce the energy consumption during peak hours of the day, Norway will implement more costly peak load tariffs and larger differences in electricity price over the hours of the day. Therefore, CTES represents a very attractive solution to tackle those peak-power costs.

For a successful integration of CTES into industrial refrigeration systems, well-designed CTES units should be applied. In this research work, the suggested CTES unit design is based on a type of HEX plates called pillow plates (PP-HEX). The novel CTES unit is shown in Fig 1. The PP-HEX consists of two metal sheets that are spot-welded together in a repeating pattern by a laser-welding machine. Fig. 2 show the surface of a finished pillow plate. An inlet and outlet pipe is then welded to the plate at each end. The inlet and outlet pipes from each plate in the stack are collected in a manifold at their respective ends of the CTES unit, serving as the connection to the external refrigeration system. Fully welding the plate edges and then applying high pressure on the inside (inflation process) completes the PP-HEX manufacturing process and creates the characteristic surface structure. The flow channels that are formed around the spot welds, allow the CO_2 to circulate on the inside and exchange heat with the PCM at the outer surface. The channel wavy shape promotes the flow mixing and thus enhances the heat transfer (Piper et al., 2016).

This is the accepted version of a paper published in 8th Conference on Ammonia and CO2 Refrigeration Technologies
DOI: 10.18462/iir.nh3-co2.2019.0041

Figure 1: The novel CTES unit

Figure 2: Surface of a PP-HEX

Until this date, published work on the heat transfer characteristics in PP-HEX is limited compared to conventional HEX types. Simple equations to describe the wavy shape of the channel geometry can generally not be used, due to the complex 3D shape of the plate surface that is created by the inflation process. Piper et al., (2015) carried out numerical metal forming simulation to identify the appropriate design parameters for PP-HEX. The simulations resulted in accurate geometric description of the PP-HEX channel cross section compared to measured values. The authors established equations for determining important geometric design parameters such as heat transfer area, hydraulic diameter and cross-sectional area. These equations are important for further developing correlations for heat transfer and pressure drop in PP-HEX.

Most of the studies of PP-HEX consider with single-phase flow. Few researches were dedicated to model the condensation/evaporation processes. Mitrovic and Peterson (2007) were the first performing experimental investigation on the condensation on PP-HEX. The condensation of isopropanol took place on the outer surface of the PP-HEX, while cooling water was flowing on the inside channels. Mitrovic and Maletic (2011) carried out numerical investigations on the flow and heat transfer characteristics of cooling water inside a PP-HEX.

Over the last few years, both numerical and experimental studies have been published on PP-HEX. Piper et. al (2016) carried out numerical investigations of the heat transfer characteristics of a periodic element (see Fig. 2) of the pillow plate. The study identified two distinct zones: the meandering core and the recirculation zone which characterize the flow inside the plate. In single-phase turbulent flow, the core flow dominates the heat transfer. The highest efficiency was observed for the lowest Reynolds numbers and the highest inflation height. It was also claimed that the PP-HEX efficiency increased by up to 37% for oval shaped welding spots compared to circular spot-weld design. In a later research work Piper et. al. (2017) established heat transfer correlations for forced convection using the CFD results. Khalil et al. (2019) investigated the effect of spot weld diameter, spot weld pitch and flow rate on the heat transfer in thermoplates, a variation of the PP-HEX with a single flow channel. In this study, the authors considered single-phase incompressible laminar flow conditions with water as the fluid. The results were experimentally validated and have shown an improvement in the heat transfer characteristics for larger spot weld spacing and smaller spot weld diameter.

In this paper, the behaviour of a PP-HEX CTES device based on the "*internal freeze/internal melt"* principle is investigated using the commercial CFD software ANSYS Fluent 19.1. Modelling solidification and melting of PCM still present challenges: crystallisation, phase segregation, degradation, supercooling and buoyancy of solid phase versus liquid phase. These are not addressed in this paper for simplification. Because water is chosen as the PCM in this study, some of these effects are not relevant, but have to be considered in futures studies of low-temperature PCMs. The CTES unit is designed to be connected into a CO_2 refrigeration cycle in a poultry processing plant. The PP-HEX can handle the high pressure of the CO_2 refrigerant. During the charging process, the water is frozen on the outside surface of the PP-HEX by CO_2 evaporation inside the plates. During the discharging process, CO_2 gas at higher temperature is circulated in the PP-HEX and condenses as it exchanges heat with the ice on the outside surface of the plate. This melts the ice from the PP-

This is the accepted version of a paper published in 8th Conference on Ammonia and CO2 Refrigeration Technologies
DOI: 10.18462/iir.nh3-co2.2019.0041

HEX surface and outwards. Literature on the ice bank systems with PP-HEX is limited. The focus of this paper is to characterize the melting/freezing process and the heat transfer characteristics between the refrigerant (CO_2) and the PCM medium (water) in the PP-HEX CTES design. The same investigation were carried out with a flat plate ice bank design and results were compared. The main findings of this research work will be later on useful to perform a full-scale CFD model of the entire CTES unit.

2. MODEL AND RESULTS

2.1. Geometry and computational domain

The dimensions of the PP-HEX are 1500 mm x 750 mm. They are horizontally stacked with 50 mm distance between each plate in the CTES unit (see Fig. 1). Two longitudinal seam welds are added to the plate to direct the refrigerant flow and ensure high utilization of the plate area. One of the seam welds is shown on the right side of Fig. 2. Creating flow passes over the plate ensures good refrigerant distribution and avoids dead zones within the plate with low heat transfer due to poor refrigerant flow. The spot welding pattern for this plate is 50 mm spacing in the longitudinal direction and 30 mm spacing in the transversal direction. The characteristic flow channels on the inside of the plate is created by blocking the outlet, and then applying high pressure with water on the inlet pipe to inflate the PP-HEX. Maximum channel height is typically in the range of 3 to 6 mm, depending on the pressure used during the inflation process and the plate thickness. The PP-HEX considered in this study has 6 mm maximum channel height. The total number plates in the stack can be varied according to the required heat transfer area of the application.

The PP-HEX plate channels are manufactured by applying a hydrostatic pressure on the inside. Due to the geometry complexity, the mathematical modelling is quite challenging and some approximation should be applied. A full size model of one PP-HEX was created using the CAD software Autodesk Inventor Professional 2019. A design approach using the tools in the software was selected to simulate the wavy surface. A small periodic element of the plate represented in Fig. 1 was cropped from the full plate geometry. The PCM is included into an enclosure of 25 mm height above the highest point of the plate surface. Geometry mirroring was applied to create the total PCM volume between two pillow plates, as shown in Fig. 2. The midsection plane between the two transversal spot welds was selected as the representative computational domain for the study, as indicated in both Fig. 1 and Fig. 2. The computational domain consists of a 30 mm wide 2D geometry, with the plate surface on the bottom and top. The shortest distance between the plates is 50 mm. Only the PCM volume is considered in this study, meaning the PP-HEX channel with the CO_2 flow is not included.

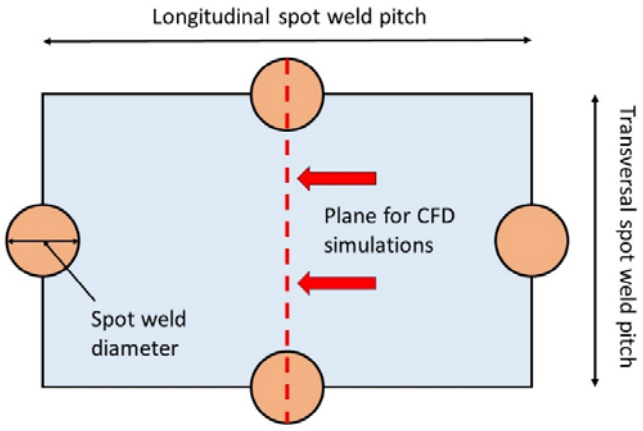

Figure 1: Top view of the periodic element of a pillow plate with domain shown

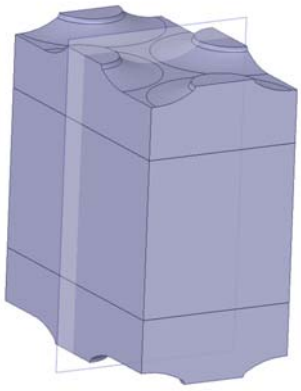

Figure 2: 3D view of the fluid volume betweeen two pillow plate with the plane section shown

One of the main aims of this study is to investigate the possibility to model the PP-HEX surface as a flat plate on the PCM side. Therefore, a 2D CFD model of two flat plates spaced by 50 mm was created. The width of the geometry is 30 mm and here again only the PCM fluid is considered in the model.

This is the accepted version of a paper published in 8th Conference on Ammonia and CO2 Refrigeration Technologies
DOI: 10.18462/iir.nh3-co2.2019.0041

2.2. The Phase Change Material

In this study, water is selected as the PCM, as its phase change temperature meets the operational range of the application. In addition, water has favourable qualities such as being non-toxic, non-flammable, having low cost and high latent heat capacity. Other applications of the CTES unit will use PCMs with solidification temperatures down to -50°C, but water is considered in this study. The thermo-physical properties of water are available in FLUENT material library. Properties such as heat capacity, density, and thermal conductivity are temperature-dependent and are defined applying user-defined functions. The relevant properties used to characterize the water are summarized in Table 1.

Table 1: Thermo-physical properties of water used in the CFD model

Property	Solid fraction	Phase change	Liquid fraction
Thermal conductivity	1.918 W m^{-1} K^{-1}	According to liquid fraction	0.579 W m^{-1} K^{-1}
Specific heat capacity	2217 J kg^{-1} K^{-1}	According to liquid fraction	4180 J kg^{-1} K^{-1}
Density	917 kg m^{-3}	Constant = liquidus property at 273.151 K	Eq.(1)
Heat of fusion		333.55 kJ kg^{-1}	
Phase change temperature		273.151 - 272.651 K (DT = 0.5K)	

2.3. Meshing of the computational domain

The computational approach of CFD requires dividing the domain into small cells where all the governing equations are solved. The meshes of the two domains in this study were created in the ANSYS Meshing software. Due to the surface shape of the PP-HEX, a fine mesh is required close to the plate surface to capture the curvature around the spot welds. A fine mesh is generally required when modelling phase change problems. In this study, a fine mesh is generated for the entire 2D domain. The pillow-plate geometry is meshed with a quad-dominant method, which is blending the triangular cells close to the plate surface to quadratic cells in the mid-region. The triangular cells are preferred in order to capture the curvature by the plate surface. Due to its simple geometry, the flat plate geometry is meshed with only quadratic elements with a typical element size of 0.5 mm. Details about the generated meshes are presented in Table 2.

Table 2: Mesh details for the two geometries

Geometry	No of elements	Minimum Orthogonal quality
Pillow plate 2D	6339	0.7425
Flat plate 2D	6000	0.9997

2.4. CFD model and boundary conditions

Two typical modelling approaches are used for phase change problems; the enthalpy-porosity model and the effective heat capacity method. In Fluent, the enthalpy-porosity formulation is generally used to track the phase change front. The interface is not tracked explicitly; a quantity called the liquid fraction is introduced. This quantity takes a value between 0 and 1 and is calculated based on the enthalpy balance of each cell. When a region is in a liquid fraction state between 0 and 1 it is treated as a porous medium, with decreasing porosity as the liquid fraction approaches zero. For more information on this model, the reader is directed to the ANSYS Fluent Theory Guide (ANSYS, 2018). This method has be proved to have good agreement with experimental results in several studies (Susman et al., 2011) (Wang et. al., 2015). The alternative method to model phase-change problems is called the effective heat capacity method. In this approach, the phase change is treated as an increase in heat capacity of the material at the phase change temperature. The peak in heat capacity corresponds to the latent heat of fusion of the material. In this work, the enthalpy-porosity model is selected.

In the current paper, investigation about the physics and heat transfer mechanism of the water freezing and melting in the temperature range of -5 to 5°C are performed. The non-linearity of water density occurring in the temperature range from 0.01°C to 10°C should be carefully modelled in order to capture its effect on the phase change process. Gebhart and Mollendorf (1977) proposed a density formulation accounting for this phenomenon, which is applicable from 0.01°C to 10.2°C. The formulation have been successfully used in several studies treating the water phase change (Scanlon and Stickland, 2004); (Shih and Chou, 2005) and is expressed as follows:

This is the accepted version of a paper published in 8th Conference on Ammonia and CO2 Refrigeration Technologies
DOI: 10.18462/iir.nh3-co2.2019.0041

$$\rho = \rho_m(1 - w|T - T_m|^q) \quad \text{Eq. (1)}$$

where ρ_m is the maximum density of water (999.972 kg m^{-3}) occurring at T_m = 4.0293°C. The constants have the values $w = 9.2793 \times 10^{-6}$ and $q = 1.894816$.

The symmetry boundary conditions are applied to the sidewalls of the domain .The top and bottom plates have constant temperatures at -5°C during the freezing process (charging cycle), which corresponds to the CO_2 evaporation pressure (P=30.47 bar). The plate temperature is 5°C (P=39.693 bar) during the melting process (discharging cycle). The thermal resistance of the plate wall is ignored. The fluid temperature of the computational domain is initialized at 5°C during the freezing process and at -5°C during the melting process. The enthalpy-porosity model is enabled only when the pressure-based solver is enabled (ANSYS, 2018). For the pressure-velocity coupling the SIMPLE scheme is applied, and for the pressure spatial discretization the PRESTO scheme is selected. For the discretization of the momentum and energy, the first order upwind method is applied. The time step is varied throughout the simulations, ranging from 0.01 seconds to 0.1 seconds after reaching stable convergence. A small time step is generally recommended to capture the phase change process, and especially because small velocities are expected in the liquid. Convergence factors for continuity, momentum and energy were selected to 10^{-4}, 10^{-4} and 10^{-8}, respectively.

2.5. Results and discussion

In this section, the simulation results of the melting (discharging) and freezing (charging) are presented. For both processes, the liquid fraction contours for pillow-plate and the flat plate models are compared, and the total plate heat transfer rates are discussed.

2.5.1. Melting/Discharging process

The liquid fraction comparison between the pillow plate and flat plate model for the melting (discharging) cycle is established for 10, 30, 60, 120, and 180 minutes and is shown in Fig. 3.

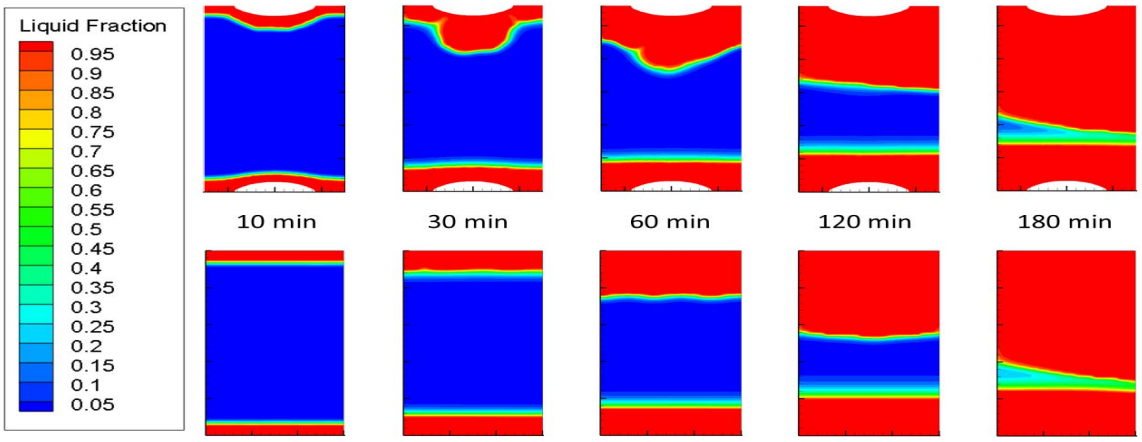

Figure 3: Comparison between the pillow-plate and the flat plate model during the melting/discharging cycle

One may note that the first layer of ice melts rapidly near the surface of the plate that has a temperature of 5°C. The density inversion effect is clearly visible, especially for the pillow plate geometry, creating a convection dominant flow between the top plate and the ice front. The water near the plate is heated, and density increases towards the maximum density point at about 4°C. This creates a single circular flow pattern of water between the cold ice and the upper heated plate. At the bottom plate the heat transfer process is dominated by conduction, as the water heated by the plate stays near the plate surface due to the maximum density occurring here. As the natural convection at the top section of the plate enhances the heat transfer, the ice melts faster in this region. This can be also clearly seen as the time progresses, the melting front moves approximately twice as fast from the top plate compared to the bottom plate. The same behaviour was observed for the flat plate configuration, but here smaller circulation patterns occurs from the top plate to the melting front. The melting process seems to progress faster in the pillow plate model compared to the flat plate for the first 30 minutes. This can be seen in Fig. 3 for the 30-minute comparison. In the region near the top plate, the liquid fraction

This is the accepted version of a paper published in 8th Conference on Ammonia and CO2 Refrigeration Technologies
DOI: 10.18462/iir.nh3-co2.2019.0041

covers a larger area for the pillow plate geometry than the flat plate geometry. As the melting process continues, the difference between the two geometries in terms of the liquid fraction reduces. The liquid fraction contour plot is close to equal after 180 minutes.

The heat transfer from the plates to the water is depicted in Fig. 4. It can be seen that the pillow plate has higher heat transfer rate during the first period, but is practically the same as for the flat plate after about 3600 seconds. The total melting time is about 11500 seconds for both geometries.

One may clearly observe the main limitation of this CFD study is that it can not capture the effect of the ice breaking loose and floating towards the top plate. The solid fraction in this study acts as if it is attached to the side boundaries, which is unphysical. The total width of the full plate is 750 mm, which means that there is adjacent fluid domains on both sides of the computational domain considered here. As the melting occurs uniformly along the total plate width, the solid ice would float upwards due to buoyancy and make contact with the top plate surface again. This effect would occur unless the ice is frozen on the vertical rods that is supporting the plates and setting the distance between them. It is in total six rods in the full-scale prototype, one in each corner, and one on each side of the plate stack. Experimental investigation of the ice behaviour during the melting cycle have to be performed to establish the dynamics of the system. It is expected that the heat transfer will increase if the ice breaks loose and makes contact with the top plate, melting the ice faster. The effect might be offset by the larger distance from the bottom plate to the melting front, as conduction is dominating that region. This behaviour should be further confirmed by experimental results.

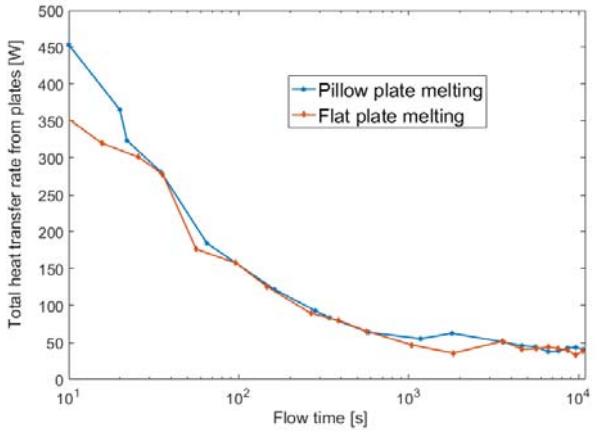

Figure 4: Total plate heat transfer rate for the melting process

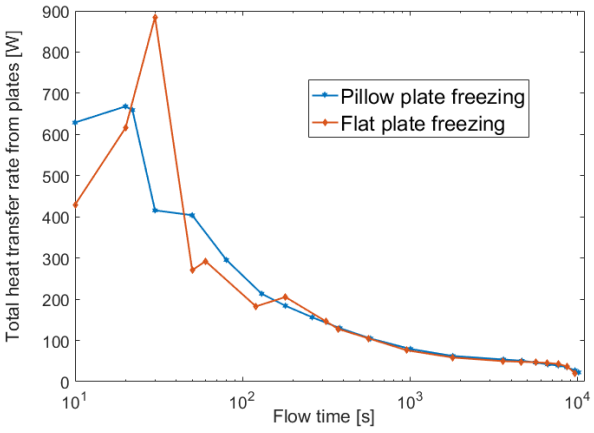

Figure 5: Total plate heat transfer rate for the freezing process

2.5.2. Freezing/Charging process

The liquid fraction comparison between the PP-HEX and flat plate configurations for the freezing (charging) process for 5, 10, 30, 60, 90, and 120 minutes are shown in Fig. 6.

As for the melting process, the heat transfer at the beginning of the phase change is high due to direct contact between the cold plate surface and the liquid water. The freezing process is faster than the melting process, mainly due to the higher thermal conductivity of the ice compared to liquid water. This can be clearly observed by comparing the 10 minutes liquid fraction contour of Fig. 3 and Fig. 6, and from the heat transfer rate calculations in Fig. 4 and Fig. 5. The heat needs to be transferred through the ice layer, and the thermal conductivity of the PCM is therefore very important. Natural convection enhances the heat transfer at the bottom ice front, but the ice layer thickness is not increasing compared to the top plate. The water near the ice is cooled and becomes less dense, inducing upward flow and creates mixing in the water between the plates. This effect seems to be more dominant for the pillow plate geometry when comparing the liquid fraction after 30 minutes of charging (see Fig. 6). This process continues until all of the liquid water has reached the freezing point temperature, where the density differences are too small to create any flow. The velocities are slowly decreasing to negligible values from 30 minutes to 60 minutes in both geometries. The heat transfer process is then purely conduction driven until the freezing process is completed. The heat transfer rates from the two

This is the accepted version of a paper published in 8th Conference on Ammonia and CO2 Refrigeration Technologies
DOI: 10.18462/iir.nh3-co2.2019.0041

plates are practically equal after 5 minutes for the pillow plate and flat plate geometry, as presented in Fig. 5. There is some fluctuation in heat transfer rate for the flat plate model during the first 60 seconds of the freezing process, shown in Fig. 5. It is suspected that this effect comes from larger velocity gradients for the flat plate model when the liquid water is cooled to the freezing point from the initial temperature of 5°C.The total freezing time is about 10200 seconds for both geometries. This suggests that modelling the pillow plate as a flat plate on the PCM side is a valid assumption for 2D domains. This will simplify future CFD studies of the unit, including full-scale models of the CTES unit.

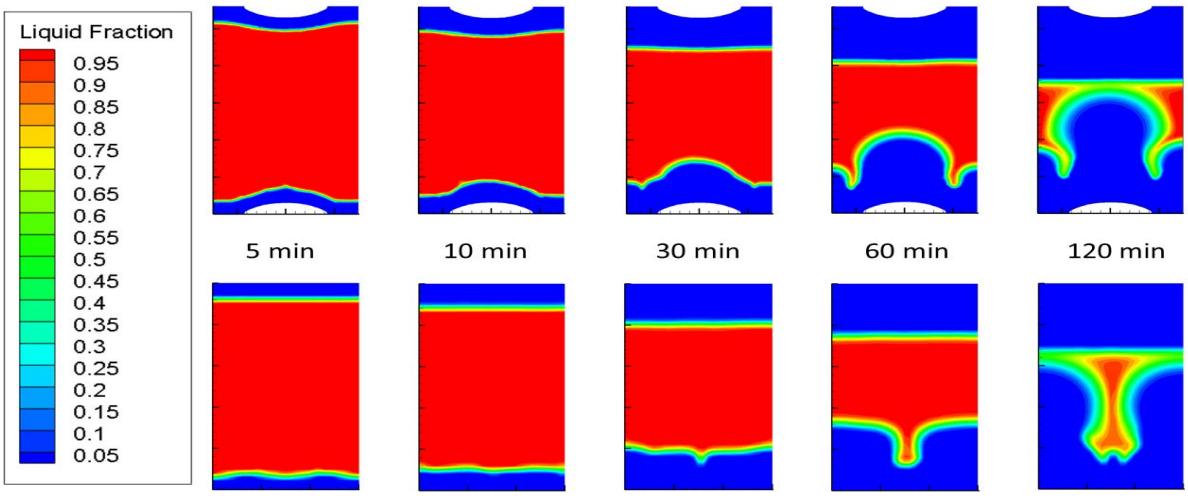

Figure 6: Comparison between the pillow-plate and the flat plate model during the freezing/charging cycle

The contours of the liquid fraction at 60 minutes and 120 minutes in Fig. 6 shows an unexpected pattern. Although the process at this time is conduction driven, the flow patterns in the fluid up to that point establish a certain shape of the ice layer. The conduction-dominant process after 60 minutes keeps the same shape of the ice layer. It is suspected that the "symmetry" boundary conditions at the sidewalls affect the flow pattern in the fluid, creating this unexpected shape of the ice layer. The symmetry boundary conditions acts as an adiabatic wall with zero shear, but is still an obstruction to flow patterns that are near the to the boundary. An additional freezing simulation with the flat plate model applying a periodic boundary condition to the sidewalls was performed. The simulation show the same evolution of the liquid fraction as for the "symmetry" condition. The periodic boundary condition makes one of the sidewalls a shadow wall of the other, so that flow out of one boundary is introduced as flow into the other boundary. In this way, the boundary does not act as an obstruction to the flow if the flow structure is larger than the domain. A larger computational domain and investigation of other boundary conditions have to be performed as future works.

CONCLUSIONS

A 2D CFD study of a novel CTES unit based on pillow-plates was performed using the commercial software Ansys FLUENT. A 2D domain of the water between two plates was selected. Both freezing and melting processes were simulated and compared to that of a flat plate configuration. The study revealed that the effect of the natural convection is important during the melting process and more dominant for the pillow plate than the flat plate during the first 30 minutes. The difference decreases as the process continues. The heat transfer rate and melting time are comparable for the two geometries. The model lacks the ability to handle the bulk ice motion when the ice breaks loose and floats to the top plate. This effect have to be further studied and investigated using an experimental setup.

The freezing cycle is faster than the melting cycle due to the higher thermal conductivity of the ice compared to liquid water. The heat transfer rates are equal for the two geometries after the first 5 minutes. The natural convection contributes to mixing the colder water near the ice front with warmer bulk fluid until it approaches the phase change temperature. After this, the freezing process is purely conduction driven. The comparison between the heat transfer rates and liquid fraction contours of the two geometries confirms that PP-HEX can

This is the accepted version of a paper published in 8th Conference on Ammonia and CO2 Refrigeration Technologies
DOI: 10.18462/iir.nh3-co2.2019.0041

be modelled as a flat plate on the PCM side in future studies. This is valid when the condition of constant plate wall temperature is used. This will greatly simplify the model when considering larger and full-scale geometries of the CTES unit.

The simulation of the freezing process reveal an unexpected contour of the liquid fraction after about 60 minutes. It is suspected that the boundary conditions on the sidewalls affect the flow pattern and creates this shape. Studies of other boundary conditions and larger domains are being investigated to deliver a more accurate model.

ACKNOWLEDGEMENTS

The work is part of HighEFF - Centre for an Energy Efficient and Competitive Industry for the Future, an 8-year Research Centre under the FME-scheme (Centre for Environment-friendly Energy Research, 257632/E20). The first author gratefully acknowledge the financial support from the Research Council of Norway and user partners of HighEFF.

REFERENCES

ANSYS, 2018. Fluent Theory Guide 19.1, Chapter 18: Solidification and Melting. ANSYS Inc

Gebhart, B. and Mollendorf, J.C., 1977. A new density relation for pure and saline water. Deep Sea Research, 24(9), pp.831-848.

Khalil, I., Hayes, R., Pratt, Q., Spitler, C. and Codd, D., 2018. Experimental and numerical modeling of heat transfer in directed thermoplates. International Journal of Heat and Mass Transfer, 123, pp.89-96.

Lorentzen, G., 1995. The use of natural refrigerants: a complete solution to the CFC/HCFC predicament. International journal of refrigeration, 18(3), pp.190-197.

Mitrovic, J. and Maletic, B., 2011. Numerical simulation of fluid flow and heat transfer in thermoplates. Chemical Engineering & Technology, 34(9), pp.1439-1448.

Mitrovic, J. and Peterson, R., 2007. Vapor condensation heat transfer in a thermoplate heat exchanger. Chemical Engineering & Technology: Industrial Chemistry-Plant Equipment-Process Engineering-Biotechnology, 30(7), pp.907-919.

Nekså, P., Walnum, H.T. and Hafner, A., 2010, April. CO2-a refrigerant from the past with prospects of being one of the main refrigerants in the future. In 9th IIR Gustav Lorentzen conference (pp. 2-14).

Piper, M., Olenberg, A., Tran, J.M. and Kenig, E.Y., 2015. Determination of the geometric design parameters of pillow-plate heat exchangers. Applied Thermal Engineering, 91, pp.1168-1175.

Piper, M., Zibart, A. and Kenig, E.Y., 2017. New design equations for turbulent forced convection heat transfer and pressure loss in pillow-plate channels. International Journal of Thermal Sciences, 120, pp.459-468.

Piper, M., Zibart, A., Tran, J.M. and Kenig, E.Y., 2016. Numerical investigation of turbulent forced convection heat transfer in pillow plates. International Journal of Heat and Mass Transfer, 94, pp.516-527.

Scanlon, T.J. and Stickland, M.T., 2004. A numerical analysis of buoyancy-driven melting and freezing. International journal of heat and mass transfer, 47(3), pp.429-436.

Shih, Y.C. and Chou, H., 2005. Numerical study of solidification around staggered cylinders in a fixed space. Numerical Heat Transfer, Part A: Applications, 48(3), pp.239-260.

Susman, G., Dehouche, Z., Cheechern, T. and Craig, S., 2011. Tests of prototype PCM ‘sails’ for office cooling. Applied Thermal Engineering, 31(5), pp.717-726.

Wang, P., Wang, X., Huang, Y., Li, C., Peng, Z. and Ding, Y., 2015. Thermal energy charging behaviour of a heat exchange device with a zigzag plate configuration containing multi-phase-change-materials (m-PCMs). Applied Energy, 142, pp.328-336.